Highlights

Dynamical Feasibility of (3) Juno as a Parent Body of the H Chondrites

John W. Noonan, Kathryn Volk, David Nesvorný, William F. Bottke

- We use dynamical modeling with the Rebound package to evaluate the ability of (3) Juno to track potential H chondrite family members for 300 Myrs after a family forming event and the TrackMet cosmic ray exposure age model to produce a synthetic cosmic ray exposure age distribution for both (3) Juno and (6) Hebe from the collisional cascade of family members.
- We find that the resulting orbital distribution of family members from a Juno family-forming event 300 Myrs ago is consistent with both the observed number of Juno family members near the 8:3J and the recent discovery of a shock-darkened H chondrite-like Near Earth Object.
- We find that the modeled cosmic ray exposure age distribution for Earth-impacting fragments from a Juno family-forming event is consistent with being drawn from the same population as the measured H chondrite cosmic ray exposure age distribution from meteorites. Fragments evolving from a similar family-forming event 300 Myrs ago (6) Hebe are statistically likely (p<0.01) to be drawn from a different distribution.

Dynamical Feasibility of (3) Juno as a Parent Body of the H Chondrites

John W. Noonan^{a,b,*}, Kathryn Volk^{a,c}, David Nesvorný^d and William F. Bottke^d

ARTICLE INFO

Keywords: Asteroids, dynamics Resonances, orbital Meteorites

ABSTRACT

We test the hypothesis that (3) Juno is a parent body of the H chondrites with dynamical modeling of an asteroid-family-forming impact and comparison to current observational data. Using a dynamical model that includes the Yarkovsky force on a simulated Juno family and a simplified cosmic ray exposure age model we examine the expected distribution of Juno family members in both the main belt and near-Earth orbits over 300 Myrs and the cosmic ray exposure distribution for fragments exiting the main belt via the 3:1J, 5:2J, and 8:3J mean motion resonances. We find that the smallest modeled ($D < 10 \, \text{m}$) family members of (3) Juno cannot be directly responsible for the observed H chondrite flux and that the breakup of larger family members creates an CRE distribution that resembles the measured H chondrites CRE distribution but is still unable to adequately explain the significant number of H chondrites with CRE ages of 6-8 Myrs. A similar model was performed for the asteroid (6) Hebe, another parent body candidate, and produced a CRE age distribution that is inconsistent with the measured H chondrite CRE ages. We also find from our dynamical models that we can expect $< 7 \, \text{km}$ -scale Juno family members in near-Earth orbits in the present day, consistent with the recent discovery of the shock-darkened H chondrite-like asteroid (52768) 1998 OR₂.

1. Introduction

Identifying the source regions of meteorites and Near-Earth Objects (NEOs) serves to improve our understanding of early solar system formation by providing traceability. By determining where the meteorites originated and how they formed we can place the structural and chemical observations of meteorites into the broader context necessary to improve the timeline of the solar system's early days (Bottke et al., 2006, 2017). Of all meteorites cataloged, 86% are classified as ordinary chondrites, and approximately 34% are H chondrites (Meteoritical Catalog, Burbine et al., 2002). H chondrites are distinct from the other large ordinary chondrite types L and LL based on their iron content (H for high, L for low, LL for very low; Burbine et al. 2002). With H chondrites representing such a large portion of meteorites for direct laboratory experiments, it is crucial to understand the dynamical feasibility of different parent bodies as their potential source.

We have some constraints on candidates for the H chondrite parent body. Early work showed spectral similarities between H chondrites and the S type asteroid (6) Hebe (Gaffey et al., 1993; Migliorini et al., 1997; Gaffey and Gilbert, 1998), but without a confirmed asteroid family to derive from, this link is tenuous (Nesvorny, 2015). The criteria that a parent body of the H chondrites must fulfill are more completely discussed in Noonan et al. (2019), but we will briefly outline them here.

Thermal modeling constraints: In an effort to constrain the size of the H chondrite parent body, thermal models based on the meteorites themselves, specifically the thermal alteration, have been implemented (Trieloff et al., 2003; Ghosh et al., 2003; Amelin et al., 2005; Blinova et al., 2007; Kleine et al., 2008; Harrison and Grimm, 2010; Henke et al., 2012; Ganguly et al., 2013; Monnereau et al., 2013; Scott et al., 2014; Blackburn et al., 2017). These studies focus on the amount of ²⁶Al heating the parent body experienced and the resulting levels of differentiation; these can be affected by the meteorite samples chosen for analysis. The majority of these efforts suggest that the H chondrite

ORCID(s): 0000-0003-2152-6987 (J.W. Noonan); 0000-0001-8736-236X (K. Volk)

^aLunar and Planetary Laboratory, University of Arizona, 1629 E University Blvd, Tucson, 85721-0092, AZ, USA

^bDepartment of Physics, Auburn University, Edmund C. Leach Science Center, Auburn, 36849, AL, USA

^cPlanetary Science Institute, 1700 East Fort Lowell, Suite 106, Tucson, 85719, AZ, USA

^d Planetary Science Directorate, Southwest Research Institute, Suite 300, 1050 Walnut St, Boulder, 80302, CO, USA

^{*}John W. Noonan

noonan@auburn.edu (J.W. Noonan)

inoons.squarespace.com (J.W. Noonan)

parent body is larger than 200 km in diameter, with the most recent study (Blackburn et al., 2017) suggesting that it was larger than 275 km.

Cosmic ray exposure ages: Of all studied H chondrites, nearly half exhibit cosmic ray exposure ages between 7 and 8 million years, a trait unique to this meteorite class (Eugster et al., 2006). Such a specific age leads us to believe that the H chondrites have one dominant parent body or collisional family, which suggests two possibilities: the parent body was located near an efficient mean motion resonance (MMR) for fast delivery of a resulting family to Earth-crossing orbits, or the body itself was near or on an Earth-crossing orbit when the breakup event happened. Both cases could result in nearly half of the H chondrites having such a distinct cosmic ray exposure age.

⁴⁰Ar-³⁹Ar Shock degassing ages: Studies of argon trapped in meteorites are useful for determining dates for significant impact events on large asteroids, specifically for impacts with resulting craters larger than 10 km in diameter. The heating from these events is large enough to go beyond the loss threshold of argon, providing a useful clue about a meteorite's parent body's impact history. For H chondrites, the ⁴⁰Ar-³⁹Ar shock degassing ages show events at 4.4-4.5, 3.5-4.1, and 0-1 billion years ago, but the largest density of ages is found at 300 million years ago (Swindle et al., 2014). This shock degassing age is in rough agreement with the estimated age of the Juno family (Nesvorny, 2015; Noonan et al., 2019).

Paleomagnetic evidence: The metallic melt impact breccia Portales Valley, an H6 meteorite (Ruzicka and Hugo, 2018a), provides evidence for a magnetic field in parent body \sim 4.5 billion years ago (Swindle et al., 2014; Bryson et al., 2016). Accretion and dynamo modeling of the parent body size to achieve the measured 10 μ T magnetic field in the sample shows that diameters between 230 and 320 km are necessary. This is consistent with the size estimates from the thermal modeling constraints.

As pointed out in Noonan et al. (2019), all of these criteria make the asteroid (3) Juno an excellent candidate for a parent body of the H chondrites. In addition, the S type surface of (3) Juno (DeMeo et al., 2009; Gaffey et al., 1993) has an 89% chance of being H chondrite-like based on a Bayesian classifier, which compares band area ratios and olivine and pyroxene abundances derived from the near-infrared spectrum of asteroids to meteoritic samples (Noonan et al., 2019). A similar spectral relationship has been reported between H chondrites and the asteroid (6) Hebe (Farinella et al., 1993; Migliorini et al., 1997; Gaffey and Gilbert, 1998; Fieber-Beyer and Gaffey, 2020), which has more favorable access to the ν6 and 3:1 MMR with Jupiter (hereafter we will use 'J' to indicate Jupiter's MMRs, e.g., 3:1J). Thus, the difficulty lies in the delivery of Juno family members to Earth-crossing orbits (Figure 1). (3) Juno sits nearly halfway between the 3:1J and 5:2J MMRs, and quite close to the 8:3J MMR. The efficiencies of these resonances at producing Earth-crossing objects (NEOs) is contingent on many factors and needs to be numerically modeled (Gladman et al., 1997; Morbidelli and Gladman, 1998). (3) Juno is not particularly well poised to create family members that quickly reach the strong 3:1J resonance, unlike another candidate (6) Hebe (Gaffey and Gilbert, 1998; Fieber-Beyer and Gaffey, 2020). The weaker 8:3J resonance is much closer (cf. Figure 1), but is not a clear source to deliver Juno family members; its scattering efficiency has only been characterized for objects with the orbital inclinations of (1) Ceres and (2) Pallas (10.6° and 34.9°, respectively; de León et al. 2010; Todorović and Todorović 2018; Kováčová et al. 2022).

However, (3) Juno has a large associated family that could be contributing. The Juno family consists of up to 1683 known members (Nesvorny, 2015), with Knežević et al. (2014) finding a slightly different number of associated family members, 1691. The family's most recent age has been determined to be ~300 MYrs (Noonan et al., 2019), while Spoto et al. (2015) finds discordant ages for the inner and outer slopes of the family that places the age of the Juno family between 370 and 550 Myrs, with a standard deviation of ~160 Myrs. A cross check between Juno family members in the AstDyS family list (Knežević and Milani, 2003; Milani et al., 2014; Knežević et al., 2014) and the NEOWISE albedo and diameter database of Masiero et al. (2015) shows that 180 family members have pre-existing diameters and albedos measured in the near infrared. (3) Juno has an albedo of 0.238 measured by IRAS (Spoto et al., 2015), while NEOWISE reports an albedo of 0.214 (Masiero et al., 2015). The similarity in age of the Juno family and the ⁴⁰Ar-³⁹Ar shock degassing ages of H chondrites would seem to suggest a connection between the events, but the dynamical feasibility of (3) Juno as a major source of meteoritic material has never been investigated. Understanding the dynamical process of delivering Juno family members to Earth-crossing orbits, especially in terms of the efficiency and timescales, is of critical importance to understanding how reasonable (3) Juno is as a parent body candidate.

The discovery of the anisotropic re-radiation termed the Yarkovsky force and its effect on meteorite delivery to the Earth makes it clear that (3) Juno's candidicacy as an H chondrite parent body must be adequately explored to evaluate the dynamics and collisional evolution that shapes the delivery of Juno family members (Bottke et al., 2006; Vokrouhlicky and Farinella, 2000). The Yarkovsky force results from the re-radiation of solar energy from an asteroid's surface, and produces a minute acceleration that is dependent on many properties: thermal emissivity,

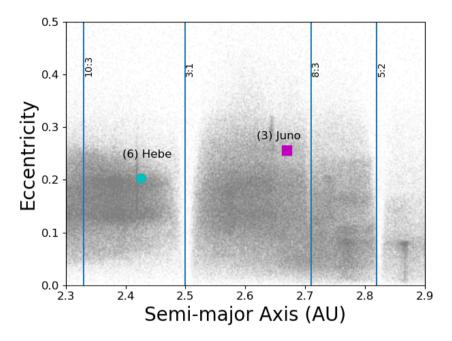


Figure 1: Plot of eccentricity vs. semi-major axis depicting (3) Juno and (6) Hebe relative to major resonances. Other main belt asteroids are plotted in grey. (6) Hebe is situated closer to the 3:1 resonance with Jupiter, but lacks a family capable of sustaining delivery of asteroids to the resonance for injection into near-Earth orbits. (3) Juno has a family, but is farther away from the strong resonance.

spin axis orientation, heliocentric distance, diameter, albedo, and so forth. The effect can happen on both diurnal and seasonal timescales, and over millenia can alter the semi-major axis of asteroids. For asteroids in the main belt this can bring them into unstable mean motion and secular resonances, scattering them into new orbits (Gladman et al., 1997; Morbidelli and Gladman, 1998; Vokrouhlicky and Farinella, 2000).

In this paper we present two models of synthetic Juno family members to address this problem. We implement a custom Yarkovsky force in the Rebound and ReboundX Python packages for dynamical integrations (Rein and Liu, 2012; Tamayo et al., 2020), as well as a collisional model to trace cosmic ray exposure ages, TrackMet, which has been previously used in Nesvorný et al. (2009) for the L chondrites. In Section 2 we describe the models and necessary assumptions. The results of the simulations are presented in Section 3 and we discuss the implications in Section 4. A summary of the paper is provided in Section 5.

2. Methods

Testing the viability of (3) Juno as the parent body of the H chondrites requires two lines of inquiry. First, the synthetic Juno family itself needs to be forward modeled to verify that the distribution of observed family members, with a recent estimated age of 300 Myrs (Noonan et al., 2019), can be achieved by gravitational and non-gravitational effects with reasonable family member albedo and emissivity assumptions. Second, cosmic ray exposure modeling is needed to confirm that a 300 Myr year old asteroid family is capable of producing a measurable flux of meteorites with a cosmic ray exposure age distribution that is nearly entirely under 10 Myrs via subsequent collisions. We have chosen dynamical modeling with the Rebound (Rein and Liu, 2012) and ReboundX (Tamayo et al., 2020) Python packages to accomplish the former and the TrackMet model (Nesvorný et al., 2009) for the latter.

2.1. Rebound Modeling

To perform the modeling of a synthetic Juno family, we used both the Rebound (Rein and Liu, 2012) and ReboundX (Tamayo et al., 2020) software packages. Integrations were performed within Rebound using both the IAS15 (Rein and Spiegel, 2015) and WHFAST (Rein and Tamayo, 2015) integrators to confirm particle behaviors were independent of integration method. Within each experimental model the Sun, Venus, Earth, Mars, Jupiter, Saturn, Uranus, and Neptune

were all added as massive bodies via calls to JPL Horizons. The orbital elements for (3) Juno are also imported and used to populate the initial state of a synthetic Juno family of asteroids.

Both the diurnal and the seasonal Yarkovsky forces are calculated at each timestep for test particles according equations 4, 5 and 6 from Bottke et al. (2006). The force is used to then calculate updated acceleration and velocity vectors for the particle within Rebound. This was accomplished by creating a new force effect using the ReboundX framework (Tamayo et al., 2020), with the full Yarkovsky force calculation added as an extra force to the Rebound simulation. We note that this was done prior to the publication of Ferich et al. (2022), who performed a similar addition that is now freely available with the ReboundX source code. We encourage readers interested in pursuing Rebound modeling of the Yarkovsky force to explore their paper and software package.

To create the synthetic Juno family asteroids, we randomly sample a position on a sphere representing (3) Juno's surface 1000 times and assign an initial velocity equal to (3) Juno's orbital velocity; we then add (3) Juno's escape velocity (120 m/s) to each particle in a direction normal to their position on the sphere (added as dv_x , dv_y , and dv_z components). This is a simplified model for a collisional family, but adequately samples the resulting potential initial orbits of family members. This family is randomly generated for each run of the simulation, allowing a wide range of initial orbital parameters to be sampled. Each family member is randomly assigned a diameter from a size frequency distribution with a power law index of -0.1. This distribution is not intended to match the size distribution of observed Juno family members, but rather to adequately explore the orbital evolution of various sizes. Each modeled family member is given a rotational period consistent with its diameter in meters, a randomized axis of rotation relative to the solar radiation, an albedo the same as (3) Juno (0.238, from IRAS and retrieved viaSpoto et al. 2015), and an emissivity of 0.005 W/m², reasonable for somewhat dust-covered S type asteroids (i.e. not a bare rock surface) (Bottke et al., 2006). The surface and bulk densities of the asteroids are assumed to be 1.7 and 2.5 g cm^3 , respectively, as detailed in Bottke et al. (2006), which are slightly smaller than the bulk density of (3) Juno, (~3.3 g cm⁻³, Viikinkoski et al. 2015).. Each of these parameters influences either the magnitude or effective direction of the Yarkovsky effect, and therefore must be assigned, or as in the case of rotation axis, randomly sampled. We note that these particle generation techniques are consistent between the Rebound and TrackMet codes to ensure comparability of results.

Following generation of this family, each particle is integrated forward in time in a system containing the massless particle, a massless (3) Juno, the terrestrial planets (except for Mercury), the gas giant planets, and the Sun. Each simulation included 100 randomly generated test particles of varying sizes, rotation rates, and initial ejection vectors from (3) Juno. The initial semi-major axes (a), eccentricities (e), and inclinations (i) of these test particles are shown in Figure 2. A cumulative distribution plot of their diameters is shown in Figure 3. Ten simulations were run simultaneously on The University of Arizona Ocelote computing cluster for a total of 200 wall time hours each. Each simulation was given 320 Myrs of total integration time, with timesteps of 0.1 years. We did not implement any collisional cascade modeling for the Rebound model; the creation of such a large number of particles would have quickly overwhelmed the dynamical simulation, unlike the one dimensional TrackMet model described in Section 2.2. To reduce computational time, we also added a conditional test particle removal check that identified test particles that reached orbits that could have close encounters with Mars or Jupiter. The conditions for this removal process are $a(1-e) \le 1.7$ au and $a(1+e) \ge 4.1$ au , where 1.7 and 4.1 au represent the semi-major axis plus/minus three times the size of the Hill radius for Mars and Jupiter, respectively.

2.2. TrackMet Modeling

To explore the collisional evolution and cosmic ray exposure ages of synthetic Juno family members, we implemented the TrackMet model described in Nesvorný et al. (2009). The model tracks the collisions for randomly generated individual family members as they evolve via the Yarkovsky effect, implemented identically to the Rebound version with the exception of timestep size, but does not execute a full dynamical model; the model only tracks radial progression in time steps of 500,000 years. Particles are collisionally evolved based on their diameters according to the rates described in Bottke et al. (2005), as in Nesvorný et al. (2009). When collisions occur, a new distribution of particles is created, conserving the mass of the original, and the model continues to track all new particles in their radial evolution. When particles evolve to sizes less than 1.5 meters in radius, the CRE age is allowed to increment within the model. Two TrackMet models are implemented to test both (3) Juno and (6) Hebe as parent sources. For (3) Juno, particles are initiated at (3) Juno's semi-major axis and evolve according the seasonal and diurnal Yarkovsky effects. If a test particle reaches the 3:1J, 5:2J, or 8:3J resonances between 298 and 302 Myrs after the family formation event, it is removed from the model and tabulated for analysis; for (6) Hebe we remove particles encountering the ν 6 and 3:1J resonances between the same times. Particles found in the 8:3J resonance are also tabulated for analysis, but

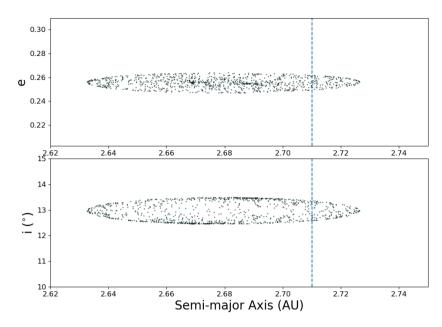


Figure 2: Initial semi-major axis, eccentricity, and inclination for randomly generated synthetic Juno family members. The 8:3J resonance is marked with a dashed line.

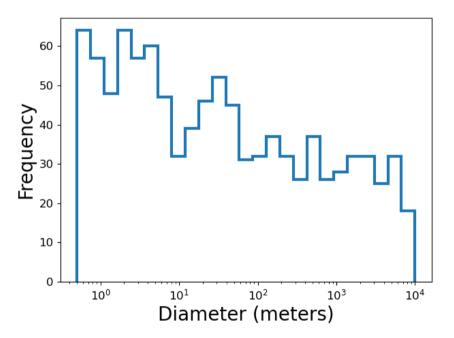


Figure 3: Histogram of randomly generated synthetic Juno family member diameters used within the Rebound model. The diameters are randomly selected from a distribution with a power law of -0.1.

are allowed to continue evolving outward to the 5:2J to improve statistics. This process is repeated for 10 million initial particles. From the particles that reach resonances with timestamps between 298 and 302 Myrs, we then sample each according to their probability of Earth impact; 0.01 for the ν 6, 2.0×10^{-3} for the 3:1J, 2.0×10^{-4} for the 5:2J (Gladman

et al., 1997; Nesvorný et al., 2009), and 1.5×10^{-4} for the 8:3J (Gladman et al., 1997; de León et al., 2010)¹. This allows us an independent method to determine the likely CRE ages of (3) Juno-derived members reaching near-Earth orbits. The lack of collisional evolution in the Rebound model makes it necessary to explore any discrepancy between TrackMet and Rebound and evaluate the limitations of each model. Such a discrepancy could indicate either a) that a specific secondary collision event is required for (3) Juno to be an adequate H chondrite source or b) (3) Juno is unlikely to be a significant source of H chondrites with the current observed properties.

3. Results

3.1. Rebound Results

A few representative particle histories from the Rebound simulations are shown in Figures 4 and 5, respectively. As expected, the smallest particles, those between 0.5 and 10 meters in size, quickly evolve to the 5:2J and 3:1J resonances before scattering, typically within 100 Myrs (Fig. 5). This evolution makes it clear that the original small members of the synthetic Juno family-forming collision ~300 Myrs ago have been effectively cleared out, with just 14% of test particles smaller than 10 m remaining, and would no longer be a significant source of H chondrite meteorites. These smaller particles also have collisional lifetimes of less than 30 Myrs (Bottke et al., 2005), far less than the total simulation time of 320 Myrs. Larger particles in the simulation, with less significant acceleration due to the Yarkovsky force, take longer to migrate into the resonances. By the end of the simulation we find that 88% of the initial 217 particles greater than 1 km in diameter are still in main belt orbits, and it is these sized objects that would have collisional lifetimes on the same timescale as the simulation. We turn our attention to these larger test particles.

A key test to underscore the validity of these simulations of the synthetic Juno family evolution is to compare the final large test particles to observed Juno family members (Figure 6). We do this comparison in proper orbital semimajor axis, eccentricity, and inclination. We use the list of observed Juno family members and their synthetic proper elements reported in the AstDyS database's family lists2 (Knežević and Milani, 2003; Milani et al., 2014; Knežević et al., 2014). For the Rebound particles, we approximate the proper elements by taking the average a,e, and i from the last 100,000 years of the simulation for each particle. While this method would not be accurate enough to determine family members from a larger main belt population, we find it is satisfactory for comparison to the AstDyS proper elements derived using a Fast Fourier Transform technique. The final semi-major axes of the D > 670 m test particles in the Rebound simulations are in good agreement with the proper elements of the observed Juno family members (see Fig. 6 caption), all of which are larger than 670 m in diameter, assuming that their albedo is similar to (3) Juno's (0.238). However, the spread of inclinations of the particles in our simulation is a little larger, which is likely the result of our uniform distribution of initial velocity vectors relative to the surface of (3) Juno. Real collisions would not likely produce such a uniform debris cloud.. These are the family members that will have collisional lifetimes of the correct scale to experience disruption near the end of the 300 Myr family age and are most likely responsible for the contributing Earth-crossing particles with CRE ages less than 20 Myrs in the complimentary TrackMet model (Farinella et al., 1998; Bottke et al., 2005). Given the model input for our synthetic family members from our simplified collision setup we are pleased with the similarity between the observed and modeled Juno family members.

3.2. TrackMet Results

The CRE ages produced by the TrackMet model provide an additional line of support for the H chondrites originating from (3) Juno. The 10 million initial particles in the TrackMet simulation are evolved collisionally and radially, and those that reach the 3:1J, 5:2J, 8:3J, and ν 6 resonances are randomly sampled 500 times with terrestrial impact probabilities of 2.0×10^{-3} , 2.0×10^{-4} , 1.5×10^{-4} and 1.0×10^{-2} , respectively, to produce averaged CRE distributions. The TrackMet code handles the terrestrial impact probabilities for the 8:3J post-simulation to allow particles evolving outwards to reach the 5:2J. The CRE age distribution of these impacts for (3) Juno is shown in the top panel of Figure 7 plotted with the actual H chondrite distribution from Marti and Graf (1992). The CRE age distribution was also modeled for family members originating from (6) Hebe, another potential candidate as a parent body for the H chondrites (Gaffey and Gilbert, 1998; Vokrouhlicky and Farinella, 2000; Fieber-Beyer and Gaffey, 2020), using the

 $^{^{1}}$ We independently tested the impact probability for particles entering the 8:3J with an inclination similar to (3) Juno via a Rebound simulation of all of the major planets and 100 test particles that we evolved for 20 Myrs. All instances where particles achieved Tisserand parameters with the Earth less than 3 were identified and collision probabilities calculated according the collision probability defined by an Öpik-algorithm based code (Öpik, 1951; Wetherill, 1967). We found that over 20 Myrs, the probability of a particle colliding with the Earth was 7.6×10^{-4} . Given that we are only removing particles between 298 and 302 Myrs in the TrackMet simulation we thus use a collision probability of 1.5×10^{-4} .

²see https://newton.spacedys.com/astdys/index.php?pc=5

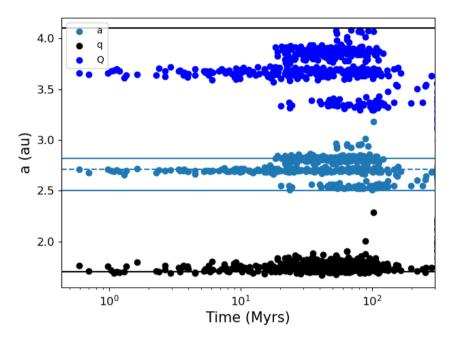


Figure 4: Semi-major axis (a), perihelion (q), and aphelion (Q) distances of particles that were removed from the simulation via intersections with Jupiter or Mars (top and bottom horizontal black lines). The 5:2 and 3:1 resonances with Jupiter are marked with the upper and lower horizontal blue lines, while the 8:3 with Jupiter is marked with a dashed blue line. Notice that the vast majority of particles were removed via interactions with Mars. Of similar interest is the apparent effectiveness of the 8:3 at scattering particles: of the 465 scattered particles, 131 had a within 0.1 au of the resonance.

v6 and 3:1J resonance and the corresponding impact probability of 1×10^{-2} for the secular v6 resonance. Due to the proximity to those resonances only 1 million initial particles are needed to obtain good statistics on particles removed between 298 and 302 Myrs. The particle creation and Yarkovsky effect are implemented identically, but the particles are given (6) Hebe's orbital parameters to start and removed when they reach the v6 and 3:1J. These two simulations allow us to directly model the expected CRE age distributions of ancient family forming impacts from (3) Juno and (6) Hebe and compare them to the measured H chondrite CRE age distribution.

Figure 7 shows that the observed H chondrite distribution is difficult to match directly. The (3) Juno distribution has a broad peak that is consistent with the H chondrite distribution, albeit lacking the steep peak at 7-8 Myrs. However, the TrackMet model makes it clear that the (6) Hebe distribution is a poor match, with a CRE peak near 3 Myrs, rather than the 7-8 Myrs seen in the measured H chondrite distribution; the (6) Hebe model over predicts the number of H chondrites that would be expected to have CRE ages under 20 Myrs. The source of the discrepancy can be traced to two factors: distance from the parent asteroids to the nearest resonance and the associated efficiency of that resonance for delivering earth impactors (Fig. 8. The order-of-magnitude higher efficiency of the ν 6 resonance compared to the 3:1J, in addition to (6) Hebe's close proximity to both, means that a large number of family members can be delivered to Earth-crossing orbits before achieving >5 Myrs of cosmic ray exposure. In comparison, synthetic Juno family members reach the 3:1 resonance with approximately the right peak CRE age, albeit with a much broader distribution. The 8:3J contributes a significant portion of low CRE age objects, but the 5:2J only contributes a relatively small portion with a wide range of CRE ages. The sharp peak in the measured H chondrite CRE age distribution is not easily recognized as the result of one particular resonance. Our interpretation of this will be discussed further in Section 4 in the context of family forming collisions in the main belt.

To quantify the similarity between the (3) Juno and (6) Hebe TrackMet modeled CRE distributions and the actual H chondrite distribution we performed the Epps-Singleton (ES) statistical tests on randomly selected particles using the SciPy *stats* module. The Epps-Singleton test is designed to compare two populations without assuming that they are drawn from a continuous distribution, making it useful for this experiment (Epps and Singleton, 1986). For the ES test, the null hypothesis is that the two samples are drawn from the same distribution; high ES and low *p* values indicate

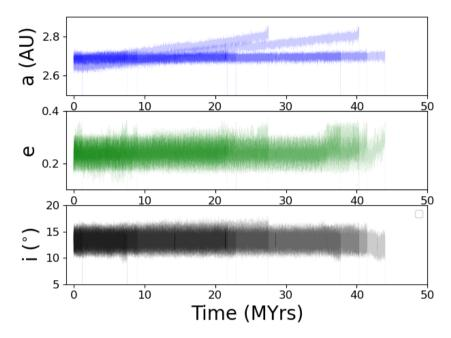


Figure 5: Evolution of semi-major axis, eccentricity, and inclination for 10 particles randomly selected from the scattered particles in the simulation. This sample all scatters within the first 50 Myrs.

that the null hypothesis can be rejected, and that the samples are drawn from different populations. We first calculate the ES value for the 431 known H chondrite CREs (Marti and Graf, 1992) compared to the entire simulated sets of Earth-crossing particles from either the (3) Juno or the (6) Hebe TrackMet models. We then bootstrap the *p*-values for these ES values by comparing subsamples of the TrackMet models to themselves. We randomly sample 431 particles from each TrackMet dataset, then calculate the ES value of that subsample compared to the overall dataset we know they were drawn from. This resampling was done 500 times, with the ES tests carried out for each resampled population, this generates the expected distribution of ES values for each modeled population to determine the likelihood of the measured H chondrite CRE ages being drawn from the same distribution as the (3) Juno/(6) Hebe CRE ages. The frequency of ES stat and bootstrapped *p*-values derived from these tests are shown in Figure 9.

When randomly sampling 431 particles from the (6) Hebe TrackMet model and comparing to the full Trackmet model, the ES test produced ES values between 0 and 115, with the majority of values smaller than 50. When comparing the measured H chondrite CRE age distribution to the (6) Hebe model we find a value of 137.78, higher than 100% of the resampled tests. This yields a bootstrapped p-value of 0, indicating that with high statistical significance a 300 Myr-old family forming event on (6) Hebe cannot reproduce the observed H chondrite CRE distribution. The same cannot be said for statistical tests of the (3) Juno TrackMet model (Figure 9). The values derived from a similar resampling of the (3) Juno dataset show a broader distribution of ES statistical values, with the ES stat limited to between 0 and 200, with the majority lower than 75. This places the ES stat calculated for the measured H chondrite distribution (20.2) smaller than 20.8% of the 500 (3) Juno subsamples, for a bootstrap p value of 0.208. We cannot reject the null hypothesis that the measured H chondrite CRE ages are drawn from the same (3) Juno resample distribution (higher p-value, lower ES stat average). As noted above, our model lacks a distinct peak between 6-8 Myrs, but the data is not statistically inconsistent with the model. We also tested the effects of removing the CRE age peak between 6-8 Myrs, which may be the result of a family member disruption, by randomly selecting only one third of the measurements between 6 and 9 Myrs. The resulting ES stat of 6.75 is smaller than 85.6% of the resampling comparisons, for a bootstrapped p-value of 0.856, which improves the match between the measured H chondrite CRE ages and those modeled from a family forming impact on (3) Juno 300 Myrs ago. We note that the Kolmogorov-Smirnov test, which assumes a continuous distribution, produces similar p-values for both the (3) Juno and (6) Hebe comparisons to the H chondrite CRE age distribution. We prefer to use the ES test since it does not require the continuous distribution assumption. While this is far from definitive, it is worth noting that the CDF of the (3) Juno TrackMet model appears to be a much better fit

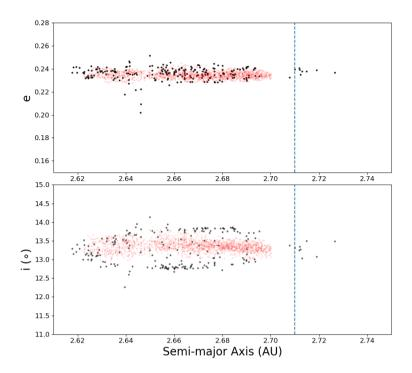


Figure 6: Comparison of the proper elements of the remaining test particles larger than 670 m in diameter in the Rebound simulation (black) with the proper elements of observed Juno family members (red). First order proper elements for the synthetic Juno family members have been determined via an average of the last 100,000 years from the Rebound simulation archive, while the proper elements for the observed Juno family members are taken from the AstDyS web portal. We find an average a,e, and i of 2.660 ± 0.024 au, 0.236 ± 0.006 , and $13.27\pm0.40^{\circ}$ for the synthetic family, in agreement with the values of 2.667 ± 0.021 au, 0.235 ± 0.003 , and $13.36\pm0.14^{\circ}$ from the AstDyS database.

at small and large CRE ages compared to (6) Hebe. The peak at 6-8 Myrs in the H chondrite CRE age distribution continues to foil attempts to model the distribution.

4. Discussion

The combination of the Rebound and TrackMet models suggests that (3) Juno's early efficiency at directly delivering primary collisional fragments to Earth-crossing orbits may be substantially supplemented by the flux of secondary objects resulting from the collisional evolution within the family. In this manner a 300 Myr old family forming event can continue to produce a meteorite population with a relatively young CRE age distribution. Given the similarity of the measured CRE distribution of H chondrites and the model, we now turn to examine the dynamical implications of (3) Juno as an H chondrite source as well as future studies to test the hypothesis.

One interesting component of the Rebound modeling is the importance of the 8:3J mean motion resonance in removing (3) Juno family members in the first 100 Myrs of the simulation. As shown in Figure 4, in the first 20 Myrs nearly all scattered particles are removed via interactions with Mars while in the 8:3J; this is consistent with the 8:3J being the first MMR that the test particles reach. Between 20 Myrs and 100 Myrs, we see the most interaction with all three resonances, and it is during this period that most of the scattered particles are removed from the Main Belt. In the last 100 Myrs of the simulation only 6 of the 1000 initial particles are scattered, and those are all the result of interactions with Mars. These last six particles are of particular interest because they represent objects that could still be on Earth-crossing orbits in the present day.

These last scattered particles are between 0.5 and 500 m in diameter, and objects larger than 300 m have a collisional lifetime on the order of their scattering lifetimes in the main belt(Bottke et al., 2005). While four of the six particles appear to have entered the 3:1J, indicating that their dynamical half-life is less than 3 Myrs in the inner solar system

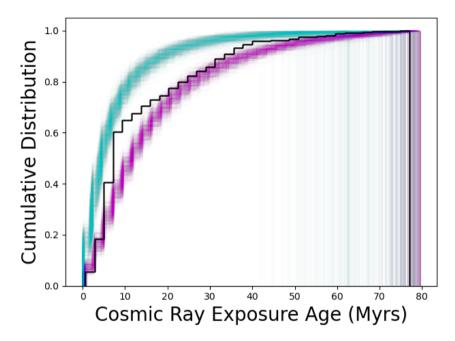


Figure 7: CRE age cumulative distributions for 500 resamplings of all Earth impacting particles originating from (3) Juno (magenta) and (6) Hebe (cyan) in the TrackMet model, with the measured H chondrite sample from Marti and Graf (1992) on Earth overlaid in black. The breakdown of impactor frequency for each resonance for (6) Hebe and (3) Juno is shown in Figure 8. Notice that the average cumulative distribution for (6) Hebe overpredicts the number of H chondrites with CRE ages under 20 Myrs. (3) Juno appears to match the measured distribution between 0 - 5 Myrs and 20 - 80 Myrs, but is depleted relative to the measured between 8 - 15 Myrs.

(Gladman et al., 1997), the most recently scattered particles are both injected into the inner solar system via the 8:3J. Unfortunately these are also small family members (D<30 m) that likely would have been disrupted within 100 Myrs of formation by the collisional evolution that is not modeled in our Rebound simulations. We note that at the end of our simulation we find ~20 (3) Juno family members very near the 8:3J resonance (Figure 6). If these simulated family members are proportional to (3) Juno's current family, then we could expect ~9% of (3) Juno's observed family population to have recently been within the 8:3J. Objects entering the inner solar system via the 8:3J have dynamical half-lives that are approximately an order of magnitude larger than those entering via the 3:1J, making it possible that large (D>300 m) Juno family members that have arrived to the 8:3J in the last 30 Myrs may still be present (Gladman et al., 1997). From that paper, and our own Rebound analysis of the 8:3J, we find that for these objects the time to enter Earth-crossing orbits is 11 Myrs on average. Given the number of observed Juno family members with D>670 m and our own fraction of (3) Juno-derived particles of similar size that have either been scattered from or recently arrived to the 8:3J in the last 30 Myrs of the simulation, we find that the presence of a large scattered Juno family member in the inner solar system should be rare in the present day. Assuming that 9% of the observed Juno family (1692 members) have passed through or are passing through the 8:3J in the last 30 Myrs, we can then calculate the number of R>335 m members remaining on an Earth-crossing orbit from the 8:3J as:

$$N_{NEO,8:3} = N_{8:3J} p_{EC} e^{-\tau^{-1} T_{EC}}$$
(1)

where the number of Juno family members over 670 m in diameter entering the 8:3J is $N_{8:3J} = 0.09 \times 1692 = 152$, $p_{EC} = 7 \times 10^{-8} \text{ yr}^{-1}$, $\tau_{EC} = 11 \text{ Myrs}$, and T = 30 Myrs. With these values we find that approximately 105 large (D>670 m) Juno family members have become Earth crossing in the last 30 Myrs and 7 can be expected to still be present in Earth crossing orbits, conservatively assuming they all entered 30 Myrs ago. This calculation depends linearly on the efficiency of Earth crossing orbits delivered from the 8:3J, so we will say that this is likely an optimistic calculation within an order of magnitude of the true value given the slow outward Yarkovsky drift of these larger family members. We note that this delivery mechanism is mentioned specifically for the 8:3J in Gladman et al. (1997).

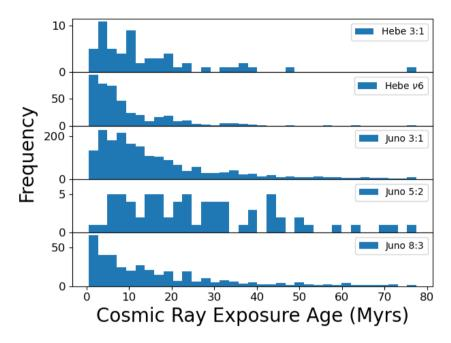


Figure 8: Contribution of each resonance to the delivery of Earth-impacting particles for (3) Juno and (6) Hebe TrackMet models. Note that the (6) Hebe CRE distribution is skewed towards younger CRE ages due to both (6) Hebe's proximity to and the high efficiency of the ν 6 resonance .

This estimate is consistent with the recent discovery of shock-darkened asteroid (52768) 1998 OR₂ (D=2.5 km) on a near-Earth orbit (Battle et al., 2022). While having a spectrum that is best classified as an Xn type in the Bus-DeMeo taxonomy (DeMeo et al., 2009), the NIR spectrum can be well fit with the reflectance spectrum of the shock-darkened H5 meteorite Chergach (Battle et al., 2022). This discovery is encouraging, indicating that there may be up to 6 more Juno-family members in the inner solar system. We note that while the presence of an NEO with an H chondrite-like spectrum is to be expected from a Juno-family forming event 300 Myrs ago, the same can not be said for a Hebe family member. Their dynamical half-life via injection into the 3:1J or ν 6 is much shorter (2.1-2.3 Myrs), making it much harder to explain large family members in near-Earth space without a larger flux of family members currently entering both resonances. Given the proximity of (6) Hebe to both the 3:1J and ν 6, even at the slower expected radial drift rates due to the Yarkovsky effect (Bottke et al., 2006) one would expect that this flux in the last 10 Myrs would be minimal. Indeed the evidence that large Hebe family members are present on both sides of the 3:1J suggests as much (Fieber-Beyer and Gaffey, 2020).

This still leaves an open question regarding the difference in the cumulative distribution functions of CRE ages for the (3) Juno model and the measured H chondrites: what is the source of the significant number of H chondrites that have a CRE age between 6-8 Myrs? While the TrackMet model is a good match to the younger (<6 Myr) and older (>8 Myr) H chondrite CRE distribution, the model is unable to explain the 6-8 Myr peak. No amount of resampling the (3) Juno TrackMet distribution could reproduce this peak, so we must hypothesize about a possible origin. A spike in 6-8 Myr H chondrites would be consistent with a catastrophic breakup of a large Juno family member just outside the 3:1J, with 1-10 m size particles drifting inwards via the Yarkovsky effect reaching the 3:1J in 2-3 Myrs, and reaching Earth-crossing orbits within another 4-5 Myrs (Gladman et al., 1997). This is not a particularly satisfying conclusion, as it requires an additional breakup event, but the collisional lifetimes of 1-2 km objects in the main belt outside of the 3:1J are on the order of 300 Myrs (Farinella et al., 1998; Bottke et al., 2005). Of course, this CRE distribution spike might not be the result of a stochastic family member breakup near the 3:1J and could instead point to a different location in the main belt for the H chondrite parent body or indicate that another separate H chondrite parent is required to properly fit the measured distribution.

One possible route to explain this is that specific spikes in the CRE age are sourced from smaller and more recent collisons on (6) Hebe, while the background H chondrite CRE distribution is sourced from the family forming impact on

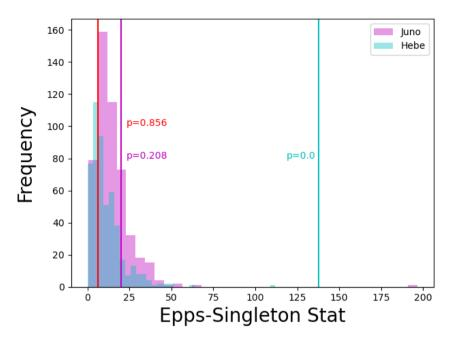


Figure 9: Epps-Singleton statistical test results for 500 subsamples of 431 particles from the modeled (3) Juno and (6) Hebe TrackMet distributions compared to their total CRE distribution. ES tests were run for each re-sampling of the TrackMet distribution to understand the likelihood of producing the known H chondrite CRE age distribution from the model. The ES values resulting from the comparison of the measured H chondrite CRE age distribution with the total (3) Juno- and (6) Hebe-sourced distributions are shown as solid magenta and cyan vertical lines, with their bootstrap *p*-values labeled. A low ES value (or high *p*-value) is consistent with being unable to reject the null hypothesis, that the two samples are drawn from the same population. The CRE ages resulting from a family forming impact on (6) Hebe 300 Myrs ago is statistically distinguishable from the H chondrite CRE age distribution, while for (3) Juno the answer is not quite as clear. The red vertical line is the ES value for comparing an H chondrite CRE age distribution that has had the 6-8 Myr peak "trimmed" to test how the removal of a recent stochastic event's contribution changes the bootstrap *p*-value. Removal of the peak increases the *p*-value by just under a factor of 4, making distinguishing between the (3) Juno-derived and measured H chondrite CRE age distributions much more difficult.

(3) Juno. Marsset et al. (2017) identified five smaller craters on (6) Hebe that could be the source of such material, and Fieber-Beyer and Gaffey (2020) linked these craters as potential sources specifically for the 6-8 Myr and 33 Myr CRE peaks in the H chondrite distribution. Such a contribution would also help to explain the relatively even distribution of H chondrite falls with orbits linked to both the 3:1J and v6 (Borovička et al., 2015). While it is possible for asteroids drifting radially to jump resonances, (i.e. Juno family members jumping the 3:1J and reaching the ν 6), the efficiency of this process is not well established (Bottke et al., 2000). This linear combination of distributions would likely be able to fit the measured one, but would introduce difficulty in explaining the widely accepted theory that the H chondrites are derived from a single major source based on isotopic and chemical evidence from the meteorite samples. This is not inconsistent with observations of the large H chondrite-like asteroids in the main belt, which appear to have all formed very rapidly and should be compositionally similar (Vernazza et al., 2014), but does still present a hurdle. Of these objects (3) Juno is the largest, which would allow the widest range of thermal processing following accretion to occur without invoking alteration for fragments after a collisional event. (3) Juno's large size make it favorable to address the variety of thermally processed H chondrites that are in the meteoritic catalog, but (6) Hebe's size is only just below the limits imposed by paleomagnetic measurements (190 km vs. 230-320 km, Ruzicka and Hugo 2018b). Clearly, future efforts to fit collisional events to observed CRE age distributions could provide more constraints on the many degeneracies of this problem, but also risk over-interpreting the available data.

If the breakup of a Juno family member or separate impacts on (6) Hebe are the source of this 6-8 Myr CRE age spike in the distribution, it may be possible to search for properties within that "spike" population that are unique compared to the broader H chondrite sample. Ideally this would mean laboratory investigations of the H chondrite samples

to search for any differences in 1 and 2 micron band depth absorption and center wavelength, yielding information about the relative abundances of olivine and pyroxene as well iron and/or calcium abundance within the minerals (Sanchez et al., 2015; Noonan et al., 2019; Fieber-Beyer and Gaffey, 2020). Such a re-analysis represents a substantial effort for NIR sample analysis, but could reveal promising clues about the origin of the H chondrite CRE age peak. Additional high resolution spectroscopy measurements of both (6) Hebe and (3) Juno to further determine differences in mineralogy are necessary to help guide new meteoritic re-analysis. The targets are eminently visible with both ground observatories, like the Legacy Survey of Space and Time planned for the Vera C. Rubin Observatory (Schwamb et al., 2023), and space-based assets, like the JWST, which can observe at new IR wavelengths (Milam et al., 2016).

5. Summary

In this work we presented dynamical models of synthetic Juno family members between 1 meter and 10 kilometers in radius. This was done to determine the viability of (3) Juno as a dominant supply of H chondrite material here on Earth given the current properties and the constraints they impose on the H chondrite parent body. We find that if we assume the 300 Myr shock degassing age of most H chondrites is indeed representative of the Juno family forming event, several conclusions can be drawn:

- 1. When only examining dynamical evolution, 14% members of the synthetic Juno family smaller than 10 meters in radius remain in main belt orbits after 300 Myrs, compared to 88% of test particles larger than 1 km in diameter.
- 2. Small (D<10 m) primary family members of (3) Juno cannot directly supply the observed H chondrite flux; the most likely source would be larger Juno family members that underwent a significant, post-family forming event collision, as evidenced by the similarity in the family age and collisional lifetime of D>300 m members.
- 3. The collisional evolution of the synthetic Juno family resulting from a family forming event 300 Myrs ago results in an Earth-crossing asteroid CRE age distribution that peaks at 6 Myrs with a significant tail at higher CRE ages. A similar (6) Hebe family forming event CRE age distribution peaks at 3 Myrs with a less significant large-age tail.
- 4. The current measured CRE age distribution of the H chondrite meteorite sample is statistically distinct from randomly drawn samples from the (6) Hebe TrackMet model. The (3) Juno TrackMet model appears to accurately represent a background H chondrite CRE age distribution. An additional source, likely a secondary breakup event 6-8 Myrs to go or discrete impacts on (6) Hebe, is necessary to explain the peak in the measured H chondrite CRE age distribution if (3) Juno is the parent body.
- 5. (6) Hebe and (3) Juno produce distinctly different CRE age distributions as parent bodies that are easily distinguished from one another.
- 6. If (3) Juno is a major parent body of the H chondrites, we can expect ∼7 asteroids in near-Earth orbits that are km-scale Juno family members at this time, consistent with the discovery of the shock-darkened asteroid (52768) 1998 OR₂ that exhibits a H chondrite like NIR spectrum.

The feasibility of (3) Juno as a parent body for the H chondrite relies heavily on the the efficiency of the 8:3J resonance to create NEOs, but it is difficult to directly model the collisional and dynamical histories of test particles simultaneously over the 300 Myr timescale with a large enough sample size to obtain good statistics. Pursuit of a more efficient method to achieve this will refine our dynamical modeling and exploration of the possible pathways to explain the observed meteorite properties and confirm parent body asteroids. We encourage the measurement of cosmic ray exposure age for newly discovered meteorites to expand the sample size for forward models to work with. A multipronged approach to understanding the lineage of the meteorite-asteroid relationship incorporating compositional and dynamical information is necessary, and a method we hope see implemented in the future.

KV acknowledges support from NASA (grants 80NSSC19K0785, 80NSSC21K0376, and 80NSSC22K0512) and NSF (grant AST-1824869). DN acknowledges support from NASA's Solar System Workings program.

References

Amelin, Y., Ghosh, A., Rotenberg, E., 2005. Unraveling the evolution of chondrite parent asteroids by precise U-Pb dating and thermal modeling. GeoCoA 69, 505–518. doi:10.1016/j.gca.2004.05.047.

Battle, A., Reddy, V., Sanchez, J.A., Sharkey, B., Pearson, N., Bowen, B., 2022. Physical Characterization of Near-Earth Asteroid (52768) 1998 OR2: Evidence of Shock Darkening/Impact Melt. PSJ 3, 226. doi:10.3847/PSJ/ac7223, arXiv:2210.03049.

- Blackburn, T., Alexander, C.M.O., Carlson, R., Elkins-Tanton, L.T., 2017. The accretion and impact history of the ordinary chondrite parent bodies. GeoCoA 200, 201–217. doi:10.1016/j.gca.2016.11.038.
- Blinova, A., Amelin, Y., Samson, C., 2007. Constraints on the cooling history of the H-chondrite parent body from phosphate and chondrule Pb-isotopic dates from Estacado. Meteoritics and Planetary Science 42, 1337–1350. doi:10.1111/j.1945-5100.2007.tb00578.x.
- Borovička, J., Spurný, P., Brown, P., 2015. Small Near-Earth Asteroids as a Source of Meteorites, in: Asteroids IV, pp. 257–280. doi:10.2458/azu_uapress_9780816532131-ch014.
- Bottke, William F., J., Vokrouhlický, D., Rubincam, D.P., Nesvorný, D., 2006. The Yarkovsky and Yorp Effects: Implications for Asteroid Dynamics. Annual Review of Earth and Planetary Sciences 34, 157–191. doi:10.1146/annurev.earth.34.031405.125154.
- Bottke, W., Mazrouei, S., Ghent, R., Parker, A., 2017. What Really Happened to Earth's Older Craters?, in: AAS/Division for Planetary Sciences Meeting Abstracts #49, p. 100.03.
- Bottke, W.F., Durda, D.D., Nesvorný, D., Jedicke, R., Morbidelli, A., Vokrouhlický, D., Levison, H.F., 2005. Linking the collisional history of the main asteroid belt to its dynamical excitation and depletion. Icarus 179, 63–94. doi:10.1016/j.icarus.2005.05.017.
- Bottke, W.F., Durda, D.D., Nesvorný, D., Jedicke, R., Morbidelli, A., Vokrouhlický, D., Levison, H.F., 2005. Linking the collisional history of the main asteroid belt to its dynamical excitation and depletion. Icarus 179, 63–94. URL: http://www.sciencedirect.com/science/article/pii/S0019103505001958, doi:10.1016/j.icarus.2005.05.017.
- Bottke, W.F., Rubincam, D.P., Burns, J.A., 2000. Dynamical Evolution of Main Belt Meteoroids: Numerical Simulations Incorporating Planetary Perturbations and Yarkovsky Thermal Forces. Icarus 145, 301–331. doi:10.1006/icar.2000.6361.
- Bottke, W.F., Vokrouhlický, D., Rubincam, D.P., Nesvorný, D., 2006. The Yarkovsky and Yorp Effects: Implications for Asteroid Dynamics. Annual Review of Earth and Planetary Sciences 34, 157–191. doi:10.1146/annurev.earth.34.031405.125154.
- Bryson, J.F.J., Weiss, B.P., Scholl, A., Getzin, B.L., Abrahams, J.N.H., Nimmo, F., 2016. Paleomagnetic evidence for a partially differentiated H chondrite parent planetesimal, in: AGU Fall Meeting Abstracts, pp. P53D–02.
- Burbine, T.H., McCoy, T.J., Meibom, A., Gladman, B., Keil, K., 2002. Meteoritic Parent Bodies: Their Number and Identification, in: Asteroids III, pp. 653–667.
- DeMeo, F.E., Binzel, R.P., Slivan, S.M., Bus, S.J., 2009. An extension of the Bus asteroid taxonomy into the near-infrared. icarus 202, 160–180. doi:10.1016/j.icarus.2009.02.005.
- Epps, T., Singleton, K.J., 1986. An omnibus test for the two-sample problem using the empirical characteristic function. Journal of Statistical Computation and Simulation 26, 177–203.
- Eugster, O., Herzog, G.F., Marti, K., Caffee, M.W., 2006. Irradiation Records, Cosmic-Ray Exposure Ages, and Transfer Times of Meteorites. p. 829.
- Farinella, P., Gonczi, R., Froeschle, C., Froeschle, C., 1993. The Injection of Asteroid Fragments into Resonances. Icarus 101, 174–187. doi:10.1006/icar.1993.1016.
- Farinella, P., Vokrouhlický, D., Hartmann, W.K., 1998. Meteorite Delivery via Yarkovsky Orbital Drift. Icarus 132, 378-387. URL: http://www.sciencedirect.com/science/article/pii/S0019103597958723, doi:10.1006/icar.1997.5872.
- Ferich, N., Baronett, S.A., Tamayo, D., Steffen, J.H., 2022. The Yarkovsky Effect in REBOUNDx. ApJS 262, 41. doi:10.3847/1538-4365/ac8d60, arXiv:2208.09987.
- Fieber-Beyer, S.K., Gaffey, M.J., 2020. The family of (6) hebe. The Planetary Science Journal 1, 68.
- Gaffey, M.J., Bell, J.F., Brown, R.H., Burbine, T.H., Piatek, J.L., Reed, K.L., Chaky, D.A., 1993. Mineralogical Variations within the S-Type Asteroid Class. Icarus 106, 573-602. doi:10.1006/icar.1993.1194.
- Gaffey, M.J., Gilbert, S.L., 1998. Asteroid 6 Hebe: The probable parent body of the H-Type ordinary chondrites and the IIE iron meteorites. Meteoritics and Planetary Science 33, 1281–1295. doi:10.1111/j.1945-5100.1998.tb01312.x.
- Gaffey, M.J., Gilbert, S.L., 1998. Asteroid 6 Hebe: The probable parent body of the H-Type ordinary chondrites and the IIE iron meteorites. Meteoritics and Planetary Science 33, 1281–1295. doi:10.1111/j.1945-5100.1998.tb01312.x.
- Ganguly, J., Tirone, M., Chakraborty, S., Domanik, K., 2013. H-chondrite parent asteroid: A multistage cooling, fragmentation and re-accretion history constrained by thermometric studies, diffusion kinetic modeling and geochronological data. GeoCoA 105, 206–220. doi:10.1016/j.gca.2012.11.024.
- Ghosh, A., Weidenschilling, S.J., McSween, H. Y., J., 2003. Importance of the accretion process in asteroid thermal evolution: 6 Hebe as an example. Meteoritics and Planetary Science 38, 711–724. doi:10.1111/j.1945-5100.2003.tb00036.x.
- Gladman, B.J., Migliorini, F., Morbidelli, A., Zappala, V., Michel, P., Cellino, A., Froeschle, C., Levison, H.F., Bailey, M., Duncan, M., 1997. Dynamical lifetimes of objects injected into asteroid belt resonances. Science 277, 197–201. doi:10.1126/science.277.5323.197.
- Harrison, K.P., Grimm, R.E., 2010. Thermal constraints on the early history of the H-chondrite parent body reconsidered. GeoCoA 74, 5410–5423. doi:10.1016/j.gca.2010.05.034.
- Henke, S., Gail, H.P., Trieloff, M., Schwarz, W.H., Kleine, T., 2012. Thermal history modelling of the H chondrite parent body. A&A 545, A135. doi:10.1051/0004-6361/201219100, arXiv:1208.4633.
- Kleine, T., Touboul, M., Van Orman, J.A., Bourdon, B., Maden, C., Mezger, K., Halliday, A.N., 2008. Hf-W thermochronometry: Closure temperature and constraints on the accretion and cooling history of the H chondrite parent body. Earth and Planetary Science Letters 270, 106–118. doi:10.1016/j.eps1.2008.03.013.
- Knežević, Z., Milani, A., 2003. Proper element catalogs and asteroid families. A&A 403, 1165-1173. doi:10.1051/0004-6361:20030475.
- Knežević, Z., Milani, A., Cellino, A., Novaković, B., Spoto, F., Paolicchi, P., 2014. Automated Classification of Asteroids into Families at Work, in: Complex Planetary Systems, Proceedings of the International Astronomical Union, pp. 130–133. doi:10.1017/S1743921314008035.
- Kováčová, M., Kornoš, L., Matlovič, P., 2022. Possibility of transporting material from Ceres to NEO region via 8:3 MMR with Jupiter. MNRAS 509, 3842–3851. doi:10.1093/mnras/stab3268, arXiv:2111.05005.
- de León, J., Campins, H., Tsiganis, K., Morbidelli, A., Licandro, J., 2010. Origin of the near-earth asteroid phaethon and the geminids meteor shower. Astronomy & Astrophysics 513, A26.

- Marsset, M., Carry, B., Dumas, C., Hanuš, J., Viikinkoski, M., Vernazza, P., Müller, T.G., Delbo, M., Jehin, E., Gillon, M., Grice, J., Yang, B., Fusco, T., Berthier, J., Sonnett, S., Kugel, F., Caron, J., Behrend, R., 2017. 3D shape of asteroid (6) Hebe from VLT/SPHERE imaging: Implications for the origin of ordinary H chondrites. \aap 604, A64. doi:10.1051/0004-6361/201731021. _eprint: 1705.10515.
- Marti, K., Graf, T., 1992. Cosmic-ray exposure history of ordinary chondrites. Annual Review of Earth and Planetary Sciences 20, 221-243.
- Masiero, J.R., DeMeo, F.E., Kasuga, T., Parker, A.H., 2015. Asteroid Family Physical Properties, in: Asteroids IV, pp. 323–340. doi:10.2458/azu_uapress_9780816532131-ch017.
- Migliorini, F., Morbidelli, A., Zappala, V., Gladman, B.J., Bailey, M.E., Cellino, A., 1997. Vesta fragments from v6 and 3:1 resonances: Implications for V-type NEAs and HED meteorities. Meteoritics and Planetary Science 32, 903–916. doi:10.1111/j.1945-5100.1997.tb01580.x.
- Milam, S.N., Stansberry, J.A., Sonneborn, G., Thomas, C., 2016. The James Webb Space Telescope's Plan for Operations and Instrument Capabilities for Observations in the Solar System. PASP 128, 018001. doi:10.1088/1538-3873/128/959/018001, arXiv:1510.04567.
- Milani, A., Cellino, A., Knežević, Z., Novaković, B., Spoto, F., Paolicchi, P., 2014. Asteroid families classification: Exploiting very large datasets. Icarus 239, 46–73. doi:10.1016/j.icarus.2014.05.039, arXiv:1312.7702.
- Monnereau, M., Toplis, M.J., Baratoux, D., Guignard, J., 2013. Thermal history of the H-chondrite parent body: Implications for metamorphic grade and accretionary time-scales. GeoCoA 119, 302–321. doi:10.1016/j.gca.2013.05.035.
- Morbidelli, A., Gladman, B., 1998. Orbital and temporal distributions of meteorites originating in the asteroid belt. Meteoritics and Planetary Science 33, 999–1016. doi:10.1111/j.1945-5100.1998.tb01707.x.
- Morbidelli, A., Gladman, B., 1998. Orbital and temporal distributions of meteorites originating in the asteroid belt. Meteoritics and Planetary Science 33, 999–1016. doi:10.1111/j.1945-5100.1998.tb01707.x.
- Nesvorny, D., 2015. Nesvorny HCM Asteroid Families V3.0. NASA Planetary Data System, EAR-A-VARGBDET-5-NESVORNYFAM-V3.0. Nesvorny, D., 2015. Nesvorny HCM Asteroid Families V3.0. NASA Planetary Data System, EAR-A-VARGBDET-5-NESVORNYFAM-V3.0.
- Nesvorný, D., Vokrouhlický, D., Morbidelli, A., Bottke, W.F., 2009. Asteroidal source of L chondrite meteorites. 1carus 200, 698-701. doi:10.1016/j.icarus.2008.12.016.
- Noonan, J.W., Reddy, V., Harris, W.M., Bottke, W.F., Sanchez, J.A., Furfaro, R., Brown, Z., Fernandes, R., Kareta, T., Lejoly, C., Teja Nallapu, R., Niazi, H.K., Slick, L.R., Schatz, L., Sharkey, B.N.L., Springmann, A., Angle, G., Bailey, L., Acuna, D.D., Lewin, C., Marchese, K., Meshel, M., Quintero, N., Tatum, K., Wilburn, G., 2019. Search for the H Chondrite Parent Body among the Three Largest S-type Asteroids: (3) Juno, (7) Iris, and (25) Phocaea. AJ 158, 213. doi:10.3847/1538-3881/ab4813.
- Noonan, J.W., Reddy, V., Harris, W.M., Bottke, W.F., Sanchez, J.A., Furfaro, R., Brown, Z., Fernandes, R., Kareta, T., Lejoly, C., Teja Nallapu, R., Niazi, H.K., Slick, L.R., Schatz, L., Sharkey, B.N.L., Springmann, A., Angle, G., Bailey, L., Acuna, D.D., Lewin, C., Marchese, K., Meshel, M., Quintero, N., Tatum, K., Wilburn, G., 2019. Search for the H Chondrite Parent Body among the Three Largest S-type Asteroids: (3) Juno, (7) Iris, and (25) Phocaea. \aj 158, 213. doi:10.3847/1538-3881/ab4813.
- Rein, H., Liu, S.F., 2012. REBOUND: an open-source multi-purpose N-body code for collisional dynamics. A&A 537, A128. doi:10.1051/0004-6361/201118085, arXiv:1110.4876.
- Rein, H., Liu, S.F., 2012. REBOUND: an open-source multi-purpose N-body code for collisional dynamics. Astronomy & Astrophysics 537, A128. URL: http://www.aanda.org/10.1051/0004-6361/201118085, doi:10.1051/0004-6361/201118085.
- Rein, H., Spiegel, D.S., 2015. IAS15: a fast, adaptive, high-order integrator for gravitational dynamics, accurate to machine precision over a billion orbits. MNRAS 446, 1424–1437. doi:10.1093/mnras/stu2164, arXiv:1409.4779.
- Rein, H., Tamayo, D., 2015. WHFAST: a fast and unbiased implementation of a symplectic Wisdom-Holman integrator for long-term gravitational simulations. MNRAS 452, 376–388. doi:10.1093/mnras/stv1257, arXiv:1506.01084.
- Ruzicka, A.M., Hugo, R.C., 2018a. Electron backscatter diffraction (EBSD) study of seven heavily metamorphosed chondrites: Deformation systematics and variations in pre-shock temperature and post-shock annealing. GeoCoA 234, 115–147. doi:10.1016/j.gca.2018.05.014.
- Ruzicka, A.M., Hugo, R.C., 2018b. Electron backscatter diffraction (EBSD) study of seven heavily metamorphosed chondrites: Deformation systematics and variations in pre-shock temperature and post-shock annealing. GeoCoA 234, 115–147. doi:10.1016/j.gca.2018.05.014.
- Sanchez, J.A., Reddy, V., Dykhuis, M., Lindsay, S., Le Corre, L., 2015. Composition of Potentially Hazardous Asteroid (214869) 2007 PA8: An H Chondrite from the Outer Asteroid Belt. \apj 808, 93. doi:10.1088/0004-637X/808/1/93. _eprint: 1507.01008.
- Schwamb, M.E., Jones, R.L., Yoachim, P., Volk, K., Dorsey, R.C., Opitom, C., Greenstreet, S., Lister, T., Snodgrass, C., Bolin, B.T., Inno, L., Bannister, M.T., Eggl, S., Solontoi, M., Kelley, M.S.P., Jurić, M., Lin, H.W., Ragozzine, D., Bernardinelli, P.H., Chesley, S.R., Daylan, T., Ďurech, J., Fraser, W.C., Granvik, M., Knight, M.M., Lisse, C.M., Malhotra, R., Oldroyd, W.J., Thirouin, A., Ye, Q., 2023. Tuning the Legacy Survey of Space and Time (LSST) Observing Strategy for Solar System Science. ApJS 266, 22. doi:10.3847/1538-4365/acc173, arXiv:2303.02355.
- Scott, E.R.D., Krot, T.V., Goldstein, J.I., Wakita, S., 2014. Thermal and impact history of the H chondrite parent asteroid during metamorphism: Constraints from metallic Fe-Ni. GeoCoA 136, 13–37. doi:10.1016/j.gca.2014.03.038, arXiv:1404.0448.
- Spoto, F., Milani, A., Knežević, Z., 2015. Asteroid family ages. Icarus 257, 275-289. doi:10.1016/j.icarus.2015.04.041, arXiv:1504.05461.
- Swindle, T.D., Kring, D.A., Weirich, J.R., 2014. 40Ar/39Ar ages of impacts involving ordinary chondrite meteorites. Geological Society of London Special Publications 378, 333–347. doi:10.1144/SP378.6.
- Tamayo, D., Rein, H., Shi, P., Hernand ez, D.M., 2020. REBOUNDx: a library for adding conservative and dissipative forces to otherwise symplectic N-body integrations. MNRAS 491, 2885–2901. doi:10.1093/mnras/stz2870, arXiv:1908.05634.
- Todorović, N., Todorović, N., 2018. The dynamical connection between phaethon and pallas. Monthly Notices of the Royal Astronomical Society 475, 601–604.
- Trieloff, M., Jessberger, E.K., Herrwerth, I., Hopp, J., Fiéni, C., Ghélis, M., Bourot-Denise, M., Pellas, P., 2003. Structure and thermal history of the H-chondrite parent asteroid revealed by thermochronometry. Nature 422, 502–506. doi:10.1038/nature01499.
- Vernazza, P., Zanda, B., Binzel, R.P., Hiroi, T., DeMeo, F.E., Birlan, M., Hewins, R., Ricci, L., Barge, P., Lockhart, M., 2014. Multiple and Fast: The Accretion of Ordinary Chondrite Parent Bodies. ApJ 791, 120. doi:10.1088/0004-637X/791/2/120, arXiv:1405.6850.

Dynamical Feasibility of (3) Juno as a Parent Body of the H chondrites

- Viikinkoski, M., Kaasalainen, M., Ďurech, J., Carry, B., Marsset, M., Fusco, T., Dumas, C., Merline, W.J., Yang, B., Berthier, J., Kervella, P., Vernazza, P., 2015. VLT/SPHERE- and ALMA-based shape reconstruction of asteroid (3) Juno. \aap 581, L3. doi:10.1051/0004-6361/201526626.
- Vokrouhlicky, D., Farinella, P., 2000. Efficient delivery of meteorites to the Earth from a wide range of asteroid parent bodies. Nature 407, 606—. URL: http://link.gale.com/apps/doc/A188067644/AONE?u=uarizona_main&sid=zotero&xid=629da540.
- Wetherill, G.W., 1967. Collisions in the asteroid belt. Journal of Geophysical Research (1896-1977) 72, 2429–2444. URL: http://agupubs.onlinelibrary.wiley.com/doi/abs/10.1029/JZ072i009p02429, doi:10.1029/JZ072i009p02429. _eprint: https://onlinelibrary.wiley.com/doi/pdf/10.1029/JZ072i009p02429.
- Öpik, E.J., 1951. Collision Probabilities with the Planets and the Distribution of Interplanetary Matter. Proceedings of the Royal Irish Academy. Section A: Mathematical and Physical Sciences 54, 165–199. URL: https://www.jstor.org/stable/20488532. publisher: Royal Irish Academy.